

****Volume Title****
ASP Conference Series, Vol. **Volume Number**
****Author****
 © ****Copyright Year**** *Astronomical Society of the Pacific*

Structure of neutron stars with unified equations of state

A. F. Fantina¹, N. Chamel¹, J. M. Pearson² and S. Goriely¹

¹*Institut d'Astronomie et d'Astrophysique, CP-226, Université Libre de Bruxelles, 1050 Brussels, Belgium*

²*Dépt. de Physique, Université de Montréal, Montréal (Québec), H3C 3J7 Canada*

Abstract. We present a set of three unified equations of states (EoSs) based on the nuclear energy-density functional (EDF) theory. These EoSs are based on generalized Skyrme forces fitted to essentially all experimental atomic mass data and constrained to reproduce various properties of infinite nuclear matter as obtained from many-body calculations using realistic two- and three-body interactions. The structure of cold isolated neutron stars is discussed in connection with some astrophysical observations.

1. Introduction

Neutron stars, born from the catastrophic gravitational collapse of massive stars with $M \gtrsim 8M_{\odot}$ at the end point of their evolution, are among the most compact objects in the Universe. The extreme conditions encountered in their interior make their description a very challenging task. Indeed, neutron stars are expected to contain very different phases of matter, from ordinary nuclei to homogeneous nuclear matter; their core with densities exceeding several times the nuclear matter saturation density might contain additional particles like hyperons or even deconfined quarks (Haensel et al. 2007). The EDF theory allows for a consistent and computationally tractable treatment of these various phases. We have determined the global structure of neutron stars using three different *unified* EoSs based on the recently developed EDFs BSk19, BSk20 and BSk21 (Goriely et al. 2010).

2. Unified equations of state for cold neutron stars

The interior of a neutron star, assumed to be in full thermodynamic equilibrium at zero temperature, is composed of three main regions: (i) the outer crust (at densities above a few times 10^4 g cm^{-3} and below $\sim 4 \times 10^{11} \text{ g cm}^{-3}$) where nuclei arranged in a body-centered lattice coexist with a quantum gas of electrons, (ii) the inner crust where neutron-proton clusters coexist with both electrons and unbound neutrons and (iii) the liquid core (above $\sim 10^{14} \text{ g cm}^{-3}$) which consists of a uniform mixture of nucleons and leptons. No other particles will be considered here (see Chamel et al. 2012, for a discussion of the consequence of a possible phase transition in the core).

These three distinct regions are described consistently using the generalized Skyrme EDFs BSk19, BSk20 and BSk21 (Goriely et al. 2010). These EDFs were fitted to the

2149 measured masses of nuclei with N and $Z \geq 8$ given in the 2003 Atomic Mass Evaluation (Audi et al. 2003), with an rms deviation of 0.58 MeV. The masses were obtained by adding to the Hartree-Fock-Bogoliubov (HFB) energy a phenomenological Wigner term and correction term for the collective energy. The EDFs were also constrained to reproduce various properties of homogeneous nuclear matter as obtained from many-body calculations using realistic two- and three- nucleon interactions. In particular, the three different EDFs BSk19, BSk20 and BSk21, were fitted to three different neutron matter EoSs, reflecting the current lack of knowledge of the high-density behaviour of dense matter. More specifically, BSk19 (BSk21) was adjusted to the softest (stiffest) EoS of neutron matter known to us, whereas BSk20 was fitted to an EoS with an intermediate stiffness.

The EoS of the outer crust has been determined in the framework of the BPS model (Baym et al. 1971) using the latest experimental atomic masses complemented with theoretical masses obtained from our HFB mass model (see Pearson et al. 2011, for details). For the inner crust, we have applied the Thomas-Fermi method extended up to the 4th order with proton shell corrections added perturbatively via the Strutinsky integral theorem (Onsi et al. 2008; Pearson et al. 2012). This method is a high-speed approximation to the self-consistent Hartree-Fock equations. Neutron shell corrections, which are known to be much smaller than proton shell corrections (Chamel et al. 2007), have been neglected. In order to further reduce the computational work, nuclear clusters have been assumed to be spherical and the Wigner-Seitz approximation has been adopted to calculate the Coulomb energy. At high densities, these clusters are found to dissolve into a plasma of neutrons, protons, electrons and muons thus delimiting the boundary between the inner crust and the core.

3. Neutron star structure

In this Section, we discuss the global structure of cold isolated neutron stars in connection with some astrophysical observations. For this purpose, we have solved the general-relativistic Tolman-Oppenheimer-Volkoff equations with our unified EoSs BSk19-20-21 using the LORENE library*.

The gravitational redshift $z_{\text{surf}} = (1 - 2GM/Rc^2)^{-1/2} - 1$, where M is the gravitational mass and R the circumferential radius of the star, can be obtained from the identification of spectral features in the electromagnetic radiation from the surface of neutron stars. Fig. 1 shows the surface redshift as a function of M for our three EoSs BSk19-20-21. For comparison, we have also plotted the redshift predicted by the SLy4 EoS (Chabanat et al. 1997). The shaded area is prohibited by General Relativity and causality. The horizontal band bounded by dashed lines corresponds to the redshift estimated from the e^+e^- annihilation line in the spectrum of the gamma-ray burst GRB 790305b (Higdon & Lingefelter 1990). Finally, the horizontal dashed-dotted line at $z_{\text{surf}} = 0.35$ corresponds to the redshift obtained by Cottam et al. (2002) from absorption lines in the X-ray spectra of the low mass X-ray binary EXO 0748-676. The redshifts predicted by our EoSs are compatible with these observations but imply different neutron-star masses: the stiffer the EoS is, the larger is the mass for a given redshift.

*<http://www.lorene.obspm.fr>

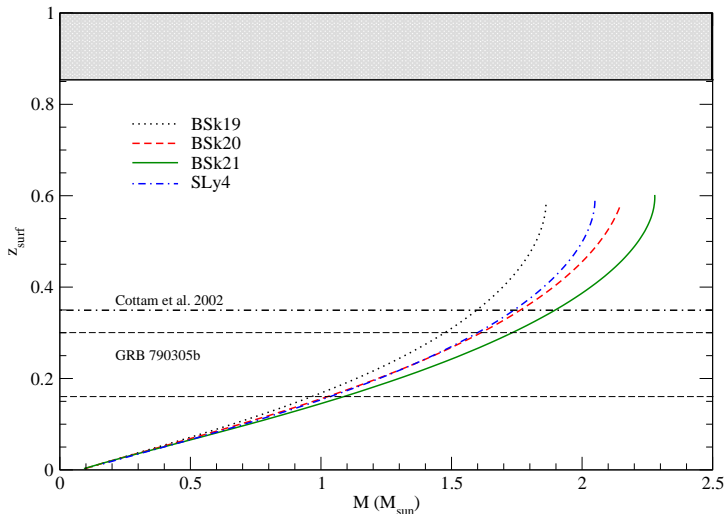


Figure 1. Gravitational surface redshift as a function of the gravitational mass for the EoSs BSk19-20-21 and SLy4.

Figure 2 shows the mass-radius relation for non-rotating stars. The horizontal band around $2M_{\odot}$ indicates the recently measured value of the mass of PSR J1614–2230 including error bars (Demorest et al. 2010). The maximum mass of neutron stars predicted by our EoS BSk19 is found to be too low, even after taking into account the effects due to the pulsar rotation (Chamel et al. 2011).

4. Conclusions

We have developed a set of three different unified EoSs of cold isolated neutron stars in the framework of the EDF theory. These EDFs are all based on generalized Skyrme forces, fitted to essentially all experimental nuclear mass data with an rms deviation falling below 0.6 MeV (Goriely et al. 2010). At the same time, these EDFs were constrained to reproduce several properties of homogeneous nuclear matter (including the neutron-matter EoS) as obtained from microscopic calculations using realistic nucleon-nucleon potentials.

These EoSs have been applied to compute the global structure of neutron stars. Even though our softest EoS BSk19 seems to be favored by measurements of the π^{-}/π^{+} production ratio in heavy-ion collision experiments (Xiao et al. 2009), it is ruled out by the recently measured mass of PSR J1614–2230 (Demorest et al. 2010). This conclusion might suggest that the dense core of neutron stars could be made of non-nucleonic matter (Chamel et al. 2012).

Acknowledgments. This work has been supported by FNRS (Belgium), NSERC (Canada) and CompStar, a Research Networking Programme of the European Science Foundation.

References

Audi, G., Wapstra, A. H., & Thibault, C. 2003, Nucl. Phys A, 729, 337

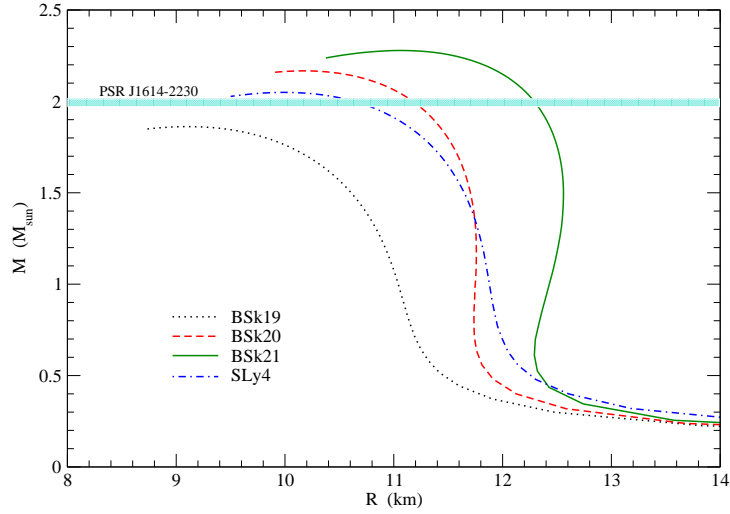


Figure 2. Gravitational mass as a functional of the circumferential radius for the EoSs BSk19-20-21 and SLy4.

- Baym, G., Pethick, C., & Sutherland, P. 1971, *ApJ*, 170, 299
 Chabamat, E., Bonche, P., Haensel, P., Meyer, J., & Schaeffer, R. 1997, *Nucl. Phys. A*, 627, 710
 Chamel, N., Fantina, A. F., Pearson, J. M., & Goriely, S. 2011, *Phys.Rev.C*, 84, 062802
 — 2012, ArXiv e-prints, 1205.0983v1
 Chamel, N., Naimi, S., Khan, E., & Margueron, J. 2007, *Phys.Rev.C*, 75
 Cottam, J., Paerels, F., & Mendez, M. 2002, *Nat*, 420, 51
 Demorest, P. B., Pennucci, T., Ransom, S. M., Roberts, M. S. E., & Hessels, J. W. T. 2010, *Nat*, 407, 1081
 Goriely, S., Chamel, N., & Pearson, J. M. 2010, *Phys.Rev.C*, 82, 035804
 Haensel, P., Potekhin, A. Y., & Yakovlev, D. G. (eds.) 2007, *Neutron Stars 1 : Equation of State and Structure*, vol. 326 of *Astrophysics and Space Science Library* (New York: Springer)
 Higdon, J. C., & Lingenfelter, R. E. 1990, *ARA&A*, 28, 401
 Onsi, M., Dutta, A. K., Chatri, H., Goriely, S., Chamel, N., & Pearson, J. M. 2008, *Phys.Rev.C*, 77, 065805
 Pearson, J. M., Chamel, N., Goriely, S., & Ducoin, C. 2012, *Phys.Rev.C*, 85, 065803
 Pearson, J. M., Goriely, S., & Chamel, N. 2011, *Phys.Rev.C*, 83, 065810
 Xiao, Z., Li, B.-A., Chen, L.-W., Yong, G.-C., & Zhang, M. 2009, *Phys.Rev.Lett*, 102, 062502